

Fast Transmission Control Adaptation for URLLC via Channel Knowledge Map and Meta-Learning

Hongsen Peng, Tobias Kallehauge, Meixia Tao, *Fellow, IEEE*, and Petar Popovski, *Fellow, IEEE*

Abstract—This paper considers methods for delivering ultra reliable low latency communication (URLLC) to enable mission-critical Internet of Things (IoT) services in wireless environments with unknown channel distribution. The methods rely upon the historical channel gain samples of a few locations in a target area. We formulate a non-trivial transmission control adaptation problem across the target area under the URLLC constraints. Then we propose two solutions to solve this problem. The *first* is a power scaling scheme in conjunction with the deep reinforcement learning (DRL) algorithm with the help of the channel knowledge map (CKM) without retraining, where the CKM employs the spatial correlation of the channel characteristics from the historical channel gain samples. The *second solution* is model agnostic meta-learning (MAML) based meta-reinforcement learning algorithm that is trained from the known channel gain samples following distinct channel distributions and can quickly adapt to the new environment within a few steps of gradient update. Simulation results indicate that the DRL-based algorithm can effectively meet the reliability requirement of URLLC under various quality-of-service (QoS) constraints. Then the adaptation capabilities of the power scaling scheme and meta-reinforcement learning algorithm are also validated.

Index Terms—URLLC, Channel Knowledge Map, Deep Reinforcement Learning, Meta-Reinforcement Learning

I. INTRODUCTION

Ultra reliable low latency communication (URLLC) is one of the main usage scenarios of 5G wireless networks and will be enhanced further to hyper reliable low latency communication (HURLLC) in 6G networks [1]–[4]. URLLC is envisioned to meet the extremely stringent quality of service (QoS) requirements so as to enable many mission-critical Internet of Things (IoT) applications, such as autonomous driving, industrial automation, unmanned aerial vehicles (UAVs) control, smart grid, etc [5]. The latency of URLLC can be generally measured by the end-to-end latency at the link layer [1], [4] (e.g. 1 ms), which takes into account both transmission delay in the physical layer and the queueing delay at the transmitter buffer in the link layer. Reliability is defined as the probability (e.g. 99.999%) that the transmitter successfully delivers a finite-size data packet to the receiver within a targeted time interval. The complement of this reliability is known as delay violation probability (DVP). This cross-layer end-to-end approach considering all the potential delay

and error sources is inevitably required for providing strong reliability and latency guarantees [2], [6]. The contradicting requirements of low latency and high reliability will bring in significant challenges in both the physical layer and the link layer of the wireless communication network [5].

At the physical layer the challenge mainly lies in the transmission outage due to the stochastic channel fading. Adaptive transmission control by exploiting instantaneous channel state information (CSI) at the transmitter is an effective approach to overcome the transmission outage and improve reliability. However, acquiring instantaneous CSI at the transmitter is difficult. On the one hand, channel estimation will bring in non-negligible latency due to pilot symbol transmission and estimated CSI feedback, which increases the overall latency and may be unacceptable for mission-critical URLLC. On the other hand, the CSI at the transmitter may not be perfect due to channel estimation error or feedback error and may also be outdated due to the rapid channel variation. Such imperfect and outdated CSI at the transmitter can significantly degrade the effectiveness of adaptive transmission control [7]. Rather than relying on instantaneous CSI acquisition, the transmission protocol can utilize statistical channel knowledge to ensure reliability and latency in a probabilistic manner [8]. In the context of ultra-reliable communication, special attention must be paid to modeling the *tail distribution* of the channel in order to capture rare events such as deep fades. Traditional parametric channel models such as Rayleigh or Rician fading may lead to severe model mismatch in the tail distribution [8], so recent works have proposed leveraging non-parametric models to avoid this problem [9].

From the link layer perspective, transmission needs to take into account queueing information. There are works that analyze DVP and delay-reliability tradeoff for URLLC wireless communication systems using various tools, such as effective capacity [10], [11], stochastic network calculus [12], extreme value theory [13] and so on. These works usually call for some specific approximations to derive corresponding tractable upper bounds. Although these bounds can provide transmission control guidance, the tightness of the bounds cannot be strictly guaranteed, resulting in low power efficiency. In addition, usually these tools require not only statistical channel knowledge as prior, but also the instantaneous CSI. In [14], we have studied a power efficient hybrid automatic repeat request (HARQ)-enabled mechanism for URLLC systems. We proposed a deep reinforcement learning (DRL) algorithm that optimizes the instantaneous coding rate and transmit power based on the queueing information and provides a tight assurance on DVP. Therein, only the statistical CSI of the

H. Peng and M. Tao are with the Department of Electronic Information and Electrical Engineering, and the Cooperative Medianet Innovation Center (CMIC), Shanghai Jiao Tong University, Shanghai, China. (Emails: {hs-peng, mxtao}@sjtu.edu.cn)

T. Kallehauge and P. Popovski are with the Department of Electronic Systems, Aalborg University, Aalborg, Denmark. (Emails: {tkal, petarp}@es.aau.dk)

environment is needed at the transmitter side.

Although relying on statistical channel knowledge can be beneficial for long-term reliability guarantees, estimating the statistics can be resource-intensive and only applies to stationary channel environment — once a user moves, the channel statistics may change and the parameters need to be re-estimated. A promising direction to acquire channel statistics with significantly fewer resources is spatial prediction. It leverages historical transmissions in a network to predict the CSI distribution directly from a user's location. Spatial prediction assumes that the long-term statistics vary smoothly in space due to shared dominant paths, scatterers, etc in the propagation environment. Thus, channel samples collected from other users in the network can, when combined with location information, be expected to predict the channel statistics at a new, yet nearby, location. Spatial prediction of channel statistics such as radio map [15], [16] is gaining increasing attention with the rise of environment-aware wireless communication for 6G networks [17] and we see a new generation of radio maps with advanced capabilities in terms of the channel knowledge map (CKM) [18], [19]. Generally speaking, CKM can be regarded as a generalization of traditional radio maps, i.e., coverage maps, which typically model the average received signal-to-noise ratio (SNR) or received signal strength in a target coverage area. This CKM also contains channel-related key information, e.g., delays/Dopplers/AoAs/AoDs of multi-paths or the complete channel impulse response. This information serves to improve environmental awareness and streamline or possibly eliminate the need for intricate real-time acquisition of CSI [18]. Regarding the channel information beyond average statistics in CKM, the work [9] introduced a novel non-parametric CKM that predicts ε -quantiles of the channel gain through the Gaussian process and proposed a rate selection algorithm for given target reliability. Note that the above CKM work [9] focuses on physical-layer adaptation only.

This work aims to exploit CKM from the cross-layer design perspective to enhance the transmission control adaptability for URLLC in mission-critical IoT systems without knowing channel distribution as prior. Motivated by the CKM works investigating the information from previously collected channel gain samples of different locations through spatial correlation, we also consider adopting meta-reinforcement learning to exploit this information and overcome the policy adaptation problem across the target area. In summary, we aim to investigate how to adapt the transmission control policy for the devices within the target area with different channel statistics while following spatial correlations. We first utilize a power scaling scheme in conjunction with DRL algorithm with the aid of the CKM constructed from the historically observed location-restricted channel gain samples. Then we employ a meta-reinforcement learning algorithm that learns an appropriate network parameter initialized from the observed channel gain samples following distinct channel distributions. This initialization can quickly adapt to the new environment within just a few gradient update steps. The main contributions of this work can be summarized as follows:

- We establish a novel framework for transmission control

adaptation problem for URLLC, aiming to minimize the long-term average transmit power while guaranteeing the QoS requirement for all the devices within the target area. Specifically, the QoS requirement is characterized as the DVP from a cross-layer design.

- We employ a power scaling algorithm in conjunction with DRL algorithm for the transmission control adaptation with the help of the CKM. Specifically, we first employ the Gaussian process (GP) to obtain the CKM of the overall target area and utilize an improved K -means clustering to divide the locations with similar channel statistics into clusters. Then we train a base DRL policy based on the location with known channel gain samples for each cluster. Finally, we conduct power scaling according to the CKM within the same cluster via CKM. Note that once all the base policies for the corresponding clusters are learned, the transmission control can achieve fast adaptation without re-training for a target area with accurate CKM.
- Then we utilize a meta-reinforcement learning algorithm that can quickly adapt to the new environment by learning from multiple location-specific environments incorporating the idea of model agnostic meta learning (MAML) without the need for CKM. The PPO-based meta-training algorithm is employed to train a policy that has good generalization capability among distinct location-specific environments. Then the meta-policy can adapt quickly to new location-specific environments with a few gradient update steps.
- Simulation results show that the PPO-based transmission control policy is efficient under various QoS requirements. Regarding the policy adaptation problem, it is also proved that the power scaling scheme and meta-DRL algorithm can guarantee the required QoS with 96.83% and 99.55% availability of the target area, respectively. The meta-DRL algorithm performs better than the power scaling scheme due to the interactions with new environments and adaptation.

The remainder of this paper is organized as follows: Section II introduces the system model and presents the formulated problem. Section III presents the DRL-based transmission control policy for a stationary environment. Section IV presents the power scaling algorithm in conjunction with the DRL-based algorithm via well-established CKM. In Section V, a meta-reinforcement learning-based algorithm is presented. Comprehensive simulation results are presented in Section VI and Section VII concludes this paper. Key notations in the system model and their definitions are summarized in Table I.

II. SYSTEM MODEL AND PROBLEM FORMULATIONS

We consider a downlink URLLC transmission scenario for mission-critical IoT services within a target area $\mathcal{Z} \in \mathbb{R}^2$ under the coverage of a base station (BS). The BS engages in communication with IoT devices (e.g., industrial actuators, robots, smart grid controller) in the target area and needs to determine the transmission parameters to meet stringent delay and reliability requirements for each device. For simplicity, the

TABLE I: Notations and definitions

Notation	Definition
\mathcal{Z}	Target area
$h(t)$	Instantaneous channel coefficient at slot t
$p(t)$	Instantaneous transmit power at slot t
$\gamma(t)$	Instantaneous channel gain at slot t
$\Gamma(t)$	Instantaneous SNR at slot t
σ_z^2	AWGN noise power
$R(t)$	Instantaneous coding rate at slot t
$A(t)$	Instantaneous arrival rate at slot t
$S(t)$	Instantaneous service rate at slot t
$Q(t)$	Queue length at slot t
$D(t)$	Delay experienced by the departure bits at slot t
ε	Outage probability for a single-shot transmission
$F_\gamma^{-1}(\varepsilon)$	ε -quantile of γ
\mathcal{D}	Channel gain data set
$1 - \xi$	Reliability target
D_{\max}	Latency target

BS and each device are assumed to have single antenna only, as our focus is on transmission control adaptation problem and learning; the presented methods can be generalized to multiple-antenna systems. It is assumed that the instantaneous CSI is unavailable at the BS side before transmission due to, e.g., low latency constraints. Therefore, the BS can only rely on statistical information of long-term channel gain samples collected from previously measured locations across the target area for transmission control.

A. Physical Layer Model

The channel coefficient from the BS to an arbitrary device in the target area, denoted as h , is assumed to follow random block fading (comprising both small-scale and large-scale fading) drawn from an *unknown distribution*, conditioned on the location of the device denoted as $\mathbf{x} \in \mathcal{Z}$. The environment including propagation, blockages and scatterers is assumed to be static during the considered communication time period. Thus the channel distribution $f(h|\mathbf{x})$ within \mathcal{Z} exhibits spatial consistency and correlation. We consider time-slotted transmission with each slot consisting of $n \in \mathbb{N}$ channel uses. The channel coefficient remains constant within each time slot and varies independently from one slot to another. The received signal at the device at slot t is modeled as

$$y(t) = \sqrt{p(t)}h(t)x(t) + z(t), \quad (1)$$

where $p(t)$ is the transmit power, $x(t)$ is the transmitted signal with unit power, and $z(t)$ is the additive white Gaussian noise (AWGN) with power $\sigma_z^2 = BN_0$ i.e., $z \sim \mathcal{CN}(0, \sigma_z^2)$, where B is the bandwidth of the channel and N_0 is the noise power spectral density. The received SNR can thus be expressed as a random variable

$$\Gamma(t) = p(t)\gamma(t) \triangleq p(t)\frac{|h(t)|^2}{\sigma_z^2}, \quad (2)$$

where $\gamma(t) \sim f(\gamma|\mathbf{x})$ denotes the effective channel gain after normalization with the noise power at slot t for location \mathbf{x} .

Due to the lack of instantaneous CSI at the BS, the effect of finite blocklength resulting from the noise instance is negligible. It is thus reasonable to work with the asymptotic outage probability with infinite blocklength [20], [21]. More

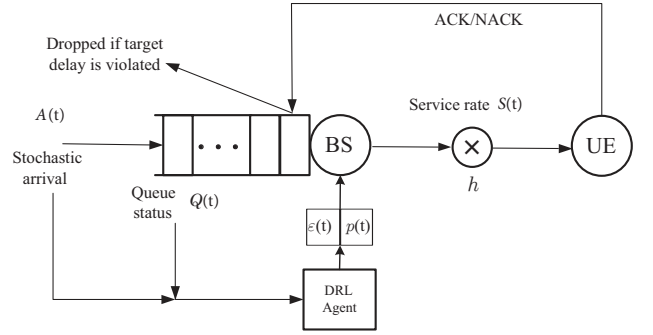


Fig. 1: Queueing diagram of the cross-layer transmission model

specifically, we consider the ε -outage capacity, i.e., the maximum rate that the channel can support with success probability $1 - \varepsilon$ to model the transmission rate between the BS and device, defined as:

$$R_\varepsilon(t) = \sup_R \{R : \Pr(\log_2(1 + \Gamma(t)) < R) < \varepsilon\}, \quad (3)$$

and can be simplified as

$$R_\varepsilon(t) = \log_2 [1 + p(t) \times F_\gamma^{-1}(\varepsilon)], \quad (4)$$

where $F_\gamma^{-1}(\varepsilon)$ is the ε -quantile of γ .

It is assumed that the explicit channel statistics of this target area are unknown to the transmitter. However, we assume that the BS has a dataset $\mathcal{D} = \{\gamma_d, \mathbf{x}_d\}_{d=1}^M$ collected over certain period from other devices across M locations \mathbf{x}_d within the same target area \mathcal{Z} . Each γ_d consists of U previously collected channel gain samples at location \mathbf{x}_d , i.e., $\gamma_d = [\gamma_d^1, \dots, \gamma_d^U]$. Here, we assume the channel process is stationary and ergodic, such that all channel gain samples at a given location are sourced from the same distribution and as long as the time duration for sample collection is long enough, these samples contain enough statistical features of the channel. It is also assumed that the long-term statistics vary smoothly in space due to shared dominant paths, scatterers, etc. In addition, the location of each device is known at the BS perfectly.

B. Link Layer Model

The link layer model depicted in Fig. 1 is similar to the one used in [22]. The overall procedures are summarized as follows: At the beginning of slot $t \in \mathbb{N}$, the data arrival rate and service rate are denoted as $A(t)$ and $S(t)$, respectively. The traffic arrival process is modeled as a stochastic process with the average arrival rate $\lambda > 0$. The BS first stores the arrived information bits in a first-in-first-out (FIFO) buffer. When each transmission is over, the device can reliably detect transmission errors and then send a one-bit error-free and delay-free acknowledgment (ACK) or negative acknowledgment (NACK) signal to inform the BS whether the transmission was successful. By neglecting these overheads and errors, we can gain an insight into the performance bounds. Upon receiving the NACK signal, the transmission is said to be in outage and the BS will retransmit the data. The data in the buffer will be dropped when an ACK signal is received, or

when the survival time of the data in the queue exceeds the target deadline, i.e., D_{\max} time slots.

According to the above mechanism, the service rate at slot t is zero when an outage occurs. Thus the service rate (in bits per slot) can be expressed as

$$S(t) = \begin{cases} 0, & \text{Outage,} \\ nR_\varepsilon(t), & \text{No outage,} \end{cases} \quad (5)$$

where $R_\varepsilon(t)$ is the coding rate at slot t , n denotes the channel uses in one slot, and

$$\Pr(\text{Outage}) = \Pr(\log_2(1 + \Gamma(t)) < R_\varepsilon(t)). \quad (6)$$

At the end of slot t , and before outdated data is dropped, the temporary queue length is given by

$$Q_{\text{tmp}}(t+1) = \max\{Q(t) + A(t) - S(t), 0\}, \quad (7)$$

where $Q(t)$ is the queue length at the beginning of slot t . If the packet has survived D_{\max} slots in the queue, the outdated data packet will be dropped. To characterize the proactive outdated data dropping, we first introduce the accumulated number of arrival bits in the latest D_{\max} slots at the end of slot t :

$$Q_{\text{th}}(t) = \sum_{i=t-D_{\max}+1}^t A(i). \quad (8)$$

Then we define the delay experienced by information bits that depart the queue at slot t as $D(t)$, and the cumulative number of delay violation events can be characterized through queue length violation events empirically as

$$\mathbb{D}(t) = \sum_{i=1}^t \mathbb{I}\{D(i) > D_{\max}\} \quad (9)$$

$$= \sum_{i=1}^t \mathbb{I}\{Q_{\text{tmp}}(i+1) > Q_{\text{th}}(i)\}, \quad (10)$$

where $\mathbb{I}\{\cdot\}$ is the indicator function.

With the proactive outdated data dropping mechanism, the queue length $Q(t+1)$ at the end of slot t after the outdated data dropping step follows that

$$Q(t+1) = \min\{Q_{\text{tmp}}(t+1), Q_{\text{th}}(t)\}. \quad (11)$$

We adopt the delay violation probability (DVP) as the performance metric related to reliability, which is defined as the probability that the actual delay $D(t)$ experienced by the bits depart the queue at slot t exceeds the maximum tolerable D_{\max} slots. Clearly, according to the above queuing mechanism, the DVP is equivalent to the queue length violation probability explicitly before outdated data dropping:

$$\Pr(D(t) > D_{\max}) = \lim_{T \rightarrow \infty} \frac{1}{T} \sum_{t=1}^T \mathbb{I}\{D(t) > D_{\max}\} \quad (12)$$

$$= \lim_{T \rightarrow \infty} \frac{1}{T} \sum_{t=1}^T \mathbb{I}\{Q_{\text{tmp}}(t+1) > Q_{\text{th}}(t)\}, \quad (13)$$

herein, the DVP is implicitly affected by the coding rate and the transmit power of each slot in the queueing system as in (7) and (11).

C. Problem Formulations

We aim to minimize the long-term average transmit power for the IoT devices while providing guaranteed reliability, i.e., bounded DVP, with a stochastic arrival process across the entire target area. To tackle this problem, we first formulate the location-specific transmission control problem by optimizing the instantaneous transmit power and coding rate with known historical channel gain samples and then formulate a transmission control adaptation problem that aims to adapt to all the locations within the target area.

For any given location \mathbf{x} with known historical channel gain samples, the power and rate control problem can be formulated as follows:

$$\min_{R(t), p(t)} \lim_{T \rightarrow \infty} \frac{1}{T} \sum_{t=1}^T p(t) \quad (14a)$$

$$\text{s.t.} \quad \Pr(D(t) > D_{\max}) \leq \xi, \quad (14b)$$

where $p(t)$ and $R(t)$ are the transmit power and the coding rate at slot t , respectively. (14b) is the target DVP constraint. The objective (14a) is the long-term average transmit power. Problem (14) is non-trivial thus we adopt a DRL-based approach to solve this problem which will be presented in detail in Section III.

Next, we generalize the location-specific problem (14) to account for all possible locations within the target area. We aim to find a transmission control adaptation policy $\Pi(\cdot|\mathbf{x})$ that can adapt to all the locations within the target area, including locations not in the dataset \mathcal{D} . We thus formulate the following problem:

$$\min_{\Pi(\cdot|\mathbf{x})} \frac{1}{|\mathcal{Z}|} \int_{\mathbf{x} \in \mathcal{Z}} \bar{P}(\mathbf{x}) d\mathbf{x} \quad (15a)$$

$$\text{s.t.} \quad \Pr(D(t) > D_{\max}|\mathbf{x}) \leq \xi, \quad \forall \mathbf{x} \in \mathcal{Z}, \quad (15b)$$

where $\bar{P}(\mathbf{x}) = \lim_{T \rightarrow \infty} \frac{1}{T} \sum_{t=1}^T p(t)$ is the long-term average transmit power concerning the channel statistics at location \mathbf{x} . Note that $\bar{P}(\mathbf{x})$ is not only related to the channel statistics of location \mathbf{x} but also related to the specified transmission control policy. Knowing the channel statistics can be utilized to determine the optimal transmission control policy and thus we omit the notation of the transmission control policy and simplify the notation as $\bar{P}(\mathbf{x})$. In problem (15), the optimization objective in (15a) is the minimum average transmit power over all the target area and the constraint in (15b) is the DVP constraint for each location within the target area. This problem is also non-trivial due to the following two aspects:

- The DVP constraints of locations without prior channel gain samples cannot be guaranteed perfectly due to the lack of statistical channel knowledge.
- The training time of the location-specific DRL algorithms for all the corresponding locations in \mathcal{D} may be prohibitively long.

We propose two solutions to solve the above policy adaptation problem (15). One is an offline power scaling approach in junction with DRL algorithm designed for (14) via a well-constructed CKM without re-training. This solution works well

for the environment with accurate CKM. The other is a meta-reinforcement learning algorithm that requires limited interaction steps with the environment when CKM is inaccurate or the new environment without CKM. The details shall be presented in Section IV and Section V, respectively.

III. LOCATION-SPECIFIC TRANSMISSION CONTROL

In this section, we employ a DRL-based algorithm to solve the power and rate control problem in (14) probabilistically for any given location \mathbf{x}_d within dataset \mathcal{D} . The policy requires selecting the transmit power $p(t)$ and outage probability $\varepsilon(t)$ with the coding rate according to the estimated ε -outage capacity:

$$R_\varepsilon(t) = \log_2(1 + p(t)\widehat{F}_\gamma^{-1}(\varepsilon(t))), \quad (16)$$

where $\widehat{F}_\gamma^{-1}(\varepsilon(t))$ is the estimated ε -quantile. Note that the traditional parametric approach for ε -quantile estimation usually assumes a parametric fading distribution, e.g., Rayleigh/Rician or Nakagami fading. This method is susceptible to model mismatch and thus influences the tail distribution of the outage probability for URLLC. In this paper, we adopt a non-parametric method for the estimation based on historically collected channel samples in \mathcal{D} .

A. Non-parametric quantile estimation

We employ a non-parametric estimator to estimate the channel gain quantiles of each location within the dataset as in [9]. For each location \mathbf{x}_d in the dataset \mathcal{D} , the ε -quantile of the channel gain, i.e., $\widehat{F}_{\gamma(\mathbf{x}_d)}^{-1}(\varepsilon)$, can be estimated from the U observations as:

$$\hat{q}_{\varepsilon,d} = \gamma_{d,(r)}, \quad r = \lfloor U\varepsilon \rfloor, \quad d = 1, \dots, M, \quad (17)$$

where $\gamma_{d,(r)}$ is the r -th order statistics of γ_d and $\lfloor \cdot \rfloor$ is the floor function that obtains the largest integer index smaller than $U\varepsilon$. To simplify the rate selection problem, we choose a discrete set of possible target outage probability levels, denoted $\mathcal{E} = \{\varepsilon_1, \dots, \varepsilon_G\}$ with G being the number of distinct outage probability levels. This generates a new data set $\mathcal{D}_\mathcal{E} = \{\hat{\mathbf{q}}_{\mathcal{E},d}, \mathbf{x}_d\}_{d=1}^M$, where $\hat{\mathbf{q}}_{\mathcal{E},d} = [\hat{q}_{\varepsilon_1,d}, \dots, \hat{q}_{\varepsilon_G,d}]$. It is worth mentioning that the quantile estimate does not require the distribution knowledge of the channel gain. Compared to parametric estimates, the main disadvantage is the excessive number of samples required for estimation when ε is small. In fact, (17) shows that U scales inversely with ε , and $\hat{q}_{\varepsilon,d}$ is only well defined when $U \geq 1/\varepsilon$. However, due to the cross-layer transmission design allowing retransmissions, to achieve the target DVP ξ , the ε -outage probability can be reduced by several orders of magnitude [23]. Thus the number of channel gain samples can also be reduced.

B. MDP formulation and DRL algorithm

For the convenience of analysis and operation, we first transform problem (14) as a Markov decision process (MDP) and divide the MDP into episodes each consisting of consecutive T slots, where one slot corresponds to a step in the MDP. Specifically, we randomly choose one sample from the U

known channel gain samples in γ_d as the channel coefficient in one slot to interact with the agent. Since we aim to use the historical channel gain samples in an offline manner and thus we randomly choose the historical channel gain samples instead of randomly generating new channel gain samples. Then we define the framework of our RL problem:

- State space: The state space \mathcal{S} is composed of the queue length information and the number of the arrived information bits. Hence the state at slot t is given by

$$s_t = \{Q(t), A(t)\}. \quad (18)$$

- Action space: The action space \mathcal{A} is composed of the outage probability and the transmit power. To ease the action tractability, we also divide the power into H discrete levels, i.e., $\mathcal{P} = \{p_1, p_2, \dots, p_H\}$ with the help of the average channel gain through \mathcal{D} , thus the action at slot t can be expressed as

$$a_t = \{\varepsilon(t), p(t)\}, \quad \forall \varepsilon(t) \in \mathcal{E}, \quad \forall p(t) \in \mathcal{P}. \quad (19)$$

- State transition function: The state transition function \mathcal{P} denotes a transition probability distribution from the current state s_t to a new state s_{t+1} after executing action a_t , i.e., $s_{t+1} \sim \Pr(\cdot | s_t, a_t)$.

$$\sum_{s_{t+1} \in \mathcal{S}} \Pr(s_{t+1} | s_t, a_t) = 1. \quad (20)$$

Note that the transition probability for a given state and an action is only related to the channel statistics in location \mathbf{x}_d and does not depend on the stochastic traffic arrival. This is because the stochastic traffic arrival in the new slot is observable at the beginning of each slot and thus can be considered deterministic. In this paper, we focus on the randomness regarding the transmission outage affected by the stochastic channel coefficient in each time slot. Thus the state transition function is determined by the channel statistics of the current location in a sense and there are two possible new states resulting from whether the transmission is in outage in (5).

- Reward function: The reward function \mathcal{R} is critical for learning the optimal transmission policy. We propose a double-layer penalty reward to capture the queue length violation probability, or equivalently, DVP as follows,

$$r_t = \begin{cases} -p(t), & Q_{\text{tmp}}(t+1) \leq Q_{\text{th}}(t) \\ -p(t) - w(t), & Q_{\text{tmp}}(t+1) > Q_{\text{th}}(t) \end{cases}, \quad (21)$$

$$w(t) = \begin{cases} \Delta \left(\frac{\mathbb{D}(t)}{T\xi^*} \right)^\nu, & \mathbb{D}(t) \leq T\xi^* \\ \Delta, & \mathbb{D}(t) > T\xi^* \end{cases}, \quad (22)$$

where Δ represents a significantly large penalty term, $T\xi^*$ denotes the target number of delay violation events which ensures the DVP and ν is a positive integer that controls the increasing speed of $w(t)$ as a function of $\mathbb{D}(t)$. Specifically, the first layer penalty depends on the latency constraint, once the equivalent queue length is violated, the penalty term emerges. However, only focusing on this penalty will result in the agent trying

$$\max_{\theta} L(\theta) = \mathbb{E}_{s_t, a_t \sim \pi_{\theta_{\text{old}}}} \left[\min \left(\frac{\pi_{\theta}(a_t|s_t)}{\pi_{\theta_{\text{old}}}(a_t|s_t)}, \text{clip} \left(\frac{\pi_{\theta}(a_t|s_t)}{\pi_{\theta_{\text{old}}}(a_t|s_t)}, 1 - \epsilon, 1 + \epsilon \right) \right) A^{\pi_{\theta_{\text{old}}}}(s_t, a_t) \right], \quad \text{clip}(x, a, b) = \begin{cases} x, & a < x < b \\ a, & x \leq a \\ b, & x \geq b \end{cases} \quad (26)$$

to not violate the target instead of ensuring $\mathbb{D}(t)$ less than the target number $T\xi^*$. Therefore, the second layer penalty term located in $w(t)$, which corresponds to the number of delay violations, is proposed.

Then we employ proximal policy optimization (PPO) [24] to solve the formulated problem due to its simplicity, sample efficiency, stability, and scalability. PPO is a policy gradient algorithm derived from the trust region policy optimization (TRPO) algorithm [25]. It can guarantee monotonically non-decreasing performance by optimizing the policy within the divergence constraint (named trust region).

We first denote the objective function of a policy π_{θ} parameterized by θ as

$$J(\theta) = \mathbb{E}_{s_0} [V_{\pi_{\theta}}(s_0)] = \mathbb{E}_{\pi_{\theta}} \left[\sum_{t=0}^T \gamma_{\text{DIS}}^t r(s_t, a_t) \right], \quad (23)$$

where γ_{DIS} is the discount factor.

Suppose the old policy $\pi_{\theta_{\text{old}}}$ is parameterized as θ_{old} . The advantage function which captures how better the current action is than the average policy can be given as

$$A^{\pi_{\theta_{\text{old}}}}(s_t, a_t) = r(s_t, a_t) + \gamma_{\text{DIS}} V_{\pi_{\theta_{\text{old}}}}(s_{t+1}) - V_{\pi_{\theta_{\text{old}}}}(s_t). \quad (24)$$

To guarantee the new policy π_{θ} performs better than the old policy $\pi_{\theta_{\text{old}}}$, we have to ensure $\mathbb{E}_{s, a \sim \pi_{\theta}} [A^{\pi_{\theta_{\text{old}}}}(s_t, a_t)] \geq 0$. It is worth mentioning that the trajectory sampled from $\pi_{\theta_{\text{old}}}$ cannot be utilized to update π_{θ} directly. To improve sample efficiency, importance sampling is proposed to deal with the new policy by utilizing the advantage functions obtained from the old policy. The policy objective substitute is optimized as follows,

$$\max_{\theta} L(\theta) = \mathbb{E}_{s, a \sim \pi_{\theta_{\text{old}}}} \left[\frac{\pi_{\theta}(a_t|s_t)}{\pi_{\theta_{\text{old}}}(a_t|s_t)} A^{\pi_{\theta_{\text{old}}}}(s_t, a_t) \right], \quad (25)$$

with Kullback-Leibler (KL) divergence constraint $\mathbb{E}[D_{\text{KL}}[\pi_{\theta}||\pi_{\theta_{\text{old}}}]] \leq D_{\text{tar}}$ between the new and old policies.

Nevertheless, the complicated KL divergence constraint involved in TRPO makes it computationally inefficient and difficult to scale up for large-scale problems. To address this problem, PPO puts the KL divergence constraint into the objective function and adopts a clipping mechanism that allows it to use a first-order optimization and thus can reduce the computational complexity significantly. The optimization problem in PPO is shown in (26) and the stochastic gradient ascent algorithm is utilized to update the network. The overall algorithm is presented in Algorithm 1.

IV. POLICY ADAPTATION VIA CHANNEL KNOWLEDGE MAP

In this section, we first establish a CKM based on the idea in [9], [26]. Then we propose a power scaling algorithm

Algorithm 1 PPO-based Algorithm

Input: Randomly initialized policy network parameters θ

for episode = 1, ..., Z **do**

$\pi_{\theta_{\text{old}}} = \pi_{\theta}$

for $t = 1, \dots, T$ **do**

Utilize $\pi_{\theta_{\text{old}}}$ to choose action a_t and interact with the environment;

Execute action a_t and receive next state s_{t+1} , reward r_t

Collect transition (s_t, a_t, r_t, s_{t+1}) to replay buffer \mathcal{B}

$s_t \leftarrow s_{t+1}$

if $t \bmod T_g = 0$ **then**

Load the transition tuples (s, a, r, s) from replay buffer \mathcal{B}

Compute the advantage function A_t based on $\pi_{\theta_{\text{old}}}$

Update the policy network by maximizing the PPO-clip objective function in (26) as: $\theta \leftarrow \theta + \alpha \nabla_{\theta} L(\theta)$

Reset the replay buffer \mathcal{B}

end if

end for

end for

based on the CKM and the trained DRL algorithm to adapt to the new location with different channel statistics without re-training. To mitigate computational complexity and improve the performance of the power scaling scheme, we also divide the locations with similar channel statistics into the same clusters for (15).

A. Channel Knowledge Map

Based on the dataset $\mathcal{D}_{\mathcal{E}}$, we will focus on the prediction of the estimated \mathcal{E} -quantiles of the new location \mathbf{x}^* that is not contained in \mathcal{D} across the target area \mathcal{Z} in the following. Firstly, we should standardize the \mathcal{E} -quantiles within $\mathcal{D}_{\mathcal{E}}$ as:

$$\hat{q}'(\mathbf{x}_d) = (\hat{q}_{\mathcal{E},d} - \bar{q})/s, \quad (27)$$

where $\bar{q} = \frac{1}{M} \sum_{d=1}^M \hat{q}_{\mathcal{E},d}$ and $s = \sqrt{\frac{1}{D} \sum_{d=1}^M (\hat{q}_{\mathcal{E},d} - \bar{q})^2}$ are the sample mean and standard deviation of the estimated \mathcal{E} -quantile $\hat{q}_{\mathcal{E},d}$ in (17) across the M locations. Based on [27], the quantile estimates derived from order statistics are asymptotically Gaussian and thus we assume the observation model $\hat{q}'_{\mathcal{E},d} = q'_{\mathcal{E},d} + \zeta$, where ζ is an independent Gaussian random variable with zero mean and variance σ_{ζ}^2 . Furthermore, it is assumed that q' is a Gaussian process [28], where $\mathbf{q}'(\mathbf{X}) = [q'(\mathbf{x}_1), \dots, q'(\mathbf{x}_M)]$ at any finite subset of locations $\mathbf{X} = [\mathbf{x}_1, \dots, \mathbf{x}_M]$ is jointly Gaussian such that

$$\mathbf{q}'(\mathbf{X}) \sim \mathcal{N}(\boldsymbol{\mu}(\mathbf{X}), \boldsymbol{\Sigma}_{\mathbf{X}\mathbf{X}}). \quad (28)$$

Here, the mean vector $\boldsymbol{\mu}(\mathbf{X}) \in \mathbb{R}^M$ is defined in terms of mean function $[\boldsymbol{\mu}(\mathbf{X})]_i = m(\mathbf{x}_i; \boldsymbol{\eta}_m)$ for $i = 1, \dots, M$ parameterized by $\boldsymbol{\eta}_m$. The elements of the covariance matrix $\boldsymbol{\Sigma}_{\mathbf{X}\mathbf{X}} \in \mathbb{R}^{M \times M}$ are given by $[\boldsymbol{\Sigma}(\mathbf{X})]_{i,j} = k(\mathbf{x}_i, \mathbf{x}_j, \boldsymbol{\eta}_k)$, where $k(\mathbf{x}_i, \mathbf{x}_j, \boldsymbol{\eta}_k)$ is a symmetric kernel function parameterized by $\boldsymbol{\eta}_k$. In the context of radio channels, the absolute exponential kernel

$$k(\mathbf{x}_i, \mathbf{x}_j; \boldsymbol{\eta}_k) = \sigma_k^2 \exp\left(-\frac{\|\mathbf{x}_i - \mathbf{x}_j\|_2}{d_c}\right), \quad (29)$$

with parameters $\boldsymbol{\eta}_k = (\sigma_k^2, d_c)$ is referred to as the Gudmundson correlations model, and has been widely applied along with a log-distance mean function to model how the average channel gain varies across space.

Note that σ_k^2 is the variance of the Gaussian process and d_c is the correlation distance, which tends to be in the order of the size of blocking objects when modeling shadow fading. As shown in [9], the Gudmundson correlation model is also well suited to model the ε -quantile of the channel gain which is therefore adopted to characterize the spatial correlation of \mathbf{q}' . For the mean, we use $m(\mathbf{x}_i) = 0$, as commonly done in Gaussian processes [28].

The CKM is constructed for a regular grid of L locations simultaneously, denoted $\mathbf{X}^* = [\mathbf{x}_1^*, \dots, \mathbf{x}_L^*]$. In order to predict the Gaussian process at locations \mathbf{X}^* , we express the joint distribution of the noisy observations $\hat{\mathbf{q}}'(\mathbf{X}) \in \mathbb{R}^M$ and quantiles in the grid $\mathbf{q}'(\mathbf{X}^*) \in \mathbb{R}^L$

$$\begin{bmatrix} \mathbf{q}'(\mathbf{X}^*) \\ \hat{\mathbf{q}}'(\mathbf{X}) \end{bmatrix} \sim \mathcal{N}\left(\mathbf{0}, \begin{bmatrix} \boldsymbol{\Sigma}_{\mathbf{X}^*\mathbf{X}^*} & \boldsymbol{\Sigma}_{\mathbf{X}^*\mathbf{X}} \\ \boldsymbol{\Sigma}_{\mathbf{X}\mathbf{X}^*} & \boldsymbol{\Sigma}_{\mathbf{X}\mathbf{X}} + \sigma_\zeta^2 \mathbf{I}_M \end{bmatrix}\right), \quad (30)$$

where $\mathbf{I}_M \in \mathbb{R}^{M \times M}$ is the identity matrix. The prediction distribution $\mathbf{q}'(\mathbf{X}^*)|\boldsymbol{\vartheta}$ is also a multivariate Gaussian distribution

$$E[\mathbf{q}'(\mathbf{X}^*)|\boldsymbol{\vartheta}] = \boldsymbol{\Sigma}_{\mathbf{X}^*\mathbf{X}}(\boldsymbol{\Sigma}_{\mathbf{X}\mathbf{X}} + \sigma_\zeta^2 \mathbf{I}_M)^{-1} \hat{\mathbf{q}}'(\mathbf{X}), \quad (31)$$

$$\text{Cov}[\mathbf{q}'(\mathbf{X}^*)|\boldsymbol{\vartheta}] = \boldsymbol{\Sigma}_{\mathbf{X}^*\mathbf{X}^*} - \boldsymbol{\Sigma}_{\mathbf{X}^*\mathbf{X}}(\boldsymbol{\Sigma}_{\mathbf{X}\mathbf{X}} + \sigma_\zeta^2 \mathbf{I}_M)^{-1} \boldsymbol{\Sigma}_{\mathbf{X}\mathbf{X}^*}, \quad (32)$$

where $\boldsymbol{\vartheta} = (\hat{\mathbf{q}}'(\mathbf{X}^*), \mathbf{X}, \mathbf{X}^*, \boldsymbol{\eta}_k)$. Equations (31) and (32) constitute the predictive distribution for $\mathbf{q}'(\mathbf{X}^*)$ and are referred to as the predictive mean and covariance, respectively. This model produces a full distribution of the predicted quantiles. For simplicity, we will directly utilize the mean value as the predicted ε -quantile regardless of the uncertainty of the estimates. The main reason is two-fold: Firstly, when conducting the coding rate and transmit power in the virtual environment with estimated ε -quantiles and the true environment with uncertainty in the ε -quantiles, the difference between the two corresponding outage probabilities in a single time slot is quite small due to the increased outage probability caused by cross-layer design [23]. Secondly, assuming the estimation error exists. When deploying the trained agent in the true environment with worse channel condition, more outage transmissions are likely to occur. As long as the queue length is long enough, the trained agent will adapt the transmission strategy to be more conservative, leading to a choice of increased coding rate and increased transmit power with a smaller outage probability, to ensure the delay violation probability; and vice versa. As a result, the above two mechanisms can alleviate the impact of the uncertainty in channel statistics.

B. Power Scaling Scheme based on CKM

In the previous section, an efficient PPO-based DRL algorithm has been utilized to solve the outage probability and power control problem in a specific location with historical channel gain samples. Here in this subsection, we aim to provide QoS guarantee for all the locations in \mathcal{Z} that do not necessarily have historical channel gain samples using the established CKM.

Intuitively, the trained PPO agent can find the optimal transmit power and outage probability in each MDP step for the specific location while guaranteeing the QoS requirement. From the state transition function perspective, this trained agent cannot efficiently guarantee the QoS for a new location with different channel statistics. When directly deploying the trained agent to a new location with better channel conditions, the agent will underestimate the channel statistics and thus will consume more transmit power than needed while the QoS requirement is met. Conversely, when deploying the trained agent to a new location with worse channel conditions, the agent will overestimate the channel statistics and the QoS requirement is more likely violated.

Thus we propose the following power scaling scheme to reduce the transmit power for the environment with better channel conditions and increase transmit power for the environment with worse channel conditions based on the established CKM. For notation simplicity, we assume $\pi_s(s_t) = \{\varepsilon(t), p_s(t)\}$, where π_s is the policy trained from the source domain, i.e., the location with known estimated quantiles $\hat{\mathbf{q}}_{\mathcal{E},s}$, and s_t is the current state observation regardless of the domain. Thus the coding rate at the source domain with state observation s_t can be expressed as

$$R_s(t) = \log_2 \left[1 + p_s(t) \times \hat{F}_{\gamma_s}^{-1}(\varepsilon(t)) \right], \quad (33)$$

where γ_s is the channel gain in the source domain. When deploying the policy π_s in the target domain, i.e., new locations with different channel statistics, with state observation s_t , we directly input the state observation s_t to the policy π_s . Then we just scale the output transmit power $p_s(t)$ according to the ε -quantile difference between the source domain and the target domain while keeping the outage probability unchanged as follows,

$$p_t(t) = p_s(t) \times \frac{\hat{F}_{\gamma_s}^{-1}(\varepsilon(t))}{\hat{F}_{\gamma_t}^{-1}(\varepsilon(t))}, \quad (34)$$

where γ_t denotes the channel gain in the target domain. This power scaling scheme can eliminate the channel statistics difference and thus guarantee that the state transition probability in the target domain is similar to the one in the source domain, i.e., similar DVP performance in a sense.

Proposition 1. *If the ε -quantiles of the source domain and the target domain satisfy $F_{\gamma_s}^{-1}(\varepsilon) = \kappa F_{\gamma_t}^{-1}(\varepsilon)$, $\forall \varepsilon \in \mathcal{E}$, κ is a constant, the optimal policy trained from the source domain after power scaling is also optimal in the target domain.*

Algorithm 2 The improved K -means clustering Algorithm

Input: Predictive quantiles in the grid $q'_{\mathcal{E}}(\mathbf{X}^*)$, the number of clusters K

Randomly choose K samples $q'_{\mathcal{E}}(\mathbf{x}_k^*)$, $1 \leq k \leq K$ from $q'_{\mathcal{E}}(\mathbf{X}^*)$ as central direction $\mu_k = q'_{\mathcal{E}}(\mathbf{x}_k^*)$

repeat

for $j = 1, \dots, L$ **do**

Compute cosine similarity between sample $q'_{\mathcal{E}}(\mathbf{x}_j^*)$ and

each central direction $\mu_k = q'_{\mathcal{E}}(\mathbf{x}_k^*)$:

$$s_{jk} = \frac{q'_{\mathcal{E}}(\mathbf{x}_j^*) \cdot q'_{\mathcal{E}}(\mathbf{x}_k^*)}{\|q'_{\mathcal{E}}(\mathbf{x}_j^*)\|_2 \times \|q'_{\mathcal{E}}(\mathbf{x}_k^*)\|_2}$$

Divide $q'_{\mathcal{E}}(\mathbf{x}_j^*)$ into cluster C_χ as:

$$\chi = \arg \max_{k=1, \dots, K} s_{jk}$$

end for

for $k = 1, \dots, K$ **do**

Compute the new central direction of each cluster as:

$$\mu'_k = \frac{1}{|C_k|} \sum_{q'_{\mathcal{E}}(\mathbf{x}_i^*) \in C_k} \frac{q'_{\mathcal{E}}(\mathbf{x}_i^*)}{\|q'_{\mathcal{E}}(\mathbf{x}_i^*)\|_2}$$

if $\mu'_k \neq \mu_k$ **do**

$$\mu_k = \mu'_k$$

else

$$\mu_k = \mu_k$$

end if

end for

until The central direction of each cluster remains constant

Output: $\{C_1, C_2, \dots, C_K\}$

Proof. The coding rates in the source domain and the target domain are

$$R_s = \log_2[1 + p_s(t)F_{\gamma_s}^{-1}(\varepsilon(t))], \quad (35)$$

$$R_t = \log_2[1 + p_t(t)F_{\gamma_t}^{-1}(\varepsilon(t))], \quad (36)$$

respectively. By substituting $F_{\gamma_t}^{-1}(\varepsilon) = \frac{1}{\kappa}F_{\gamma_s}^{-1}(\varepsilon)$ in to (36), we can obtain the coding rate in the target domain as

$$R_t = \log_2[1 + \frac{p_t(t)}{\kappa}F_{\gamma_s}^{-1}(\varepsilon(t))] \quad (37)$$

$$= \log_2[1 + \rho(t)F_{\gamma_s}^{-1}(\varepsilon(t))], \quad (38)$$

where $\rho(t) = \frac{p_t(t)}{\kappa}$. Based on (38), we can find that the state transition function of the target domain and the source domain are quite similar and the only difference lies in the parameter κ , which remains constant for all the possible ε . It can be easily proved that minimizing the average transmit power $p_t(t)$ with channel distribution $\gamma_t \sim F_{\gamma_t}(x)$ in (36) is equivalent to minimizing the average transmit power $\rho(t)$ with channel distribution $\gamma_s \sim F_{\gamma_s}(x)$ in (38) by decoupling the constant parameter κ . Thus the power scaling scheme shown in (34) is optimal when the condition $F_{\gamma_s}^{-1}(\varepsilon) = \kappa F_{\gamma_t}^{-1}(\varepsilon)$, $\forall \varepsilon \in \mathcal{E}$ holds. \square

Practically, most of the channel statistics across space can not meet the requirement $F_{\gamma_s}^{-1}(\varepsilon) = \kappa F_{\gamma_t}^{-1}(\varepsilon)$, $\forall \varepsilon \in \mathcal{E}$ strictly. There will be a mismatch among different channel distributions. To reduce computational complexity and improve the performance of the power scaling scheme, we adopt an improved K -means clustering to divide the L \mathcal{E} -quantiles of the considered grid area into K clusters. The improved K -means clustering can divide the most similar \mathcal{E} -quantiles by

cosine similarity into the same cluster, i.e., ensuring $\widehat{F}_{\gamma_s}^{-1}(\varepsilon) \approx \kappa \widehat{F}_{\gamma_t}^{-1}(\varepsilon)$, within the target area and thus reduce the power consumption resulting from channel distribution mismatch. The details of the improved K -means clustering algorithm are shown in Algorithm 2. Specifically, we first randomly choose K \mathcal{E} -quantiles as the central direction of the K clusters. Then we can compute the cosine similarity of all the other $L - K$ \mathcal{E} -quantiles with respect to the K central direction and divide the corresponding \mathcal{E} -quantiles into different clusters. Finally, we update the central direction of each cluster by averaging the normalized direction of all the \mathcal{E} -quantiles within each cluster. This algorithm terminates until the central direction of each cluster remains constant. After determining the K clusters, we need to choose K base locations from those clusters as source domains and train K agents from the K base locations respectively to ensure the effectiveness of the power scaling scheme. Once the K base policies are trained, the transmission control for any given location within the target area \mathcal{Z} can be achieved without the need for any additional training time.

V. TRANSMISSION CONTROL ADAPTATION VIA META-DRL

In the previous section, we have proposed a power scaling scheme that can provide QoS guarantee for the user located in the target area \mathcal{Z} with the help of the CKM. However, the CKM may be inaccurate since it is just a predicted map and we do not know the realistic channel statistics indeed. Thus the power scaling scheme may not work well when the predictive quantiles of the target domain are inaccurate. In this section, we propose a meta-reinforcement learning algorithm for (15) based on MAML [29] framework from a different perspective.

The core idea of MAML is to pre-train meta parameters on a large variety of different tasks and quickly adapt to a new task based on the meta parameters after a few step gradient updates. The reinforcement learning framework based on MAML, as outlined in [29], is directly applicable to our problem, given its emphasis on addressing on-policy MDP. Notably, the PPO algorithm is recognized as an on-policy reinforcement algorithm, which aligns with the scope of this approach. In the following, we will first introduce the elements of meta-reinforcement learning and then introduce the MAML-based reinforcement learning algorithm.

A. Meta-Reinforcement Learning Elements

The objective of meta-reinforcement learning is to find a model that can quickly adapt to new tasks comprising similar tasks in different environments or different tasks in the same environment. In our problem, the former is considered. We first define a meta-task set \mathcal{N} consisting of $|\mathcal{N}| = N$ tasks. Each task \mathcal{T}_i , $i \in \mathcal{N}$, denotes a long-term power minimization problem in (14) for a specific location with known channel gain samples. Thus \mathcal{T}_i can be modeled as an MDP, which is similar to the MDP expression in Section III. The key elements of the MDP also include the state space \mathcal{S} , action space \mathcal{A} , state transition function \mathcal{P} and reward function \mathcal{R} . Note that the action space in this MDP is reformulated as the coding rate and the transmit power directly without the need for channel

gain samples and the corresponding ε -quantiles in advance. More specifically, the known channel gain samples of this given location will be utilized to interact with the agent for task \mathcal{T}_i . The main objective of this agent is to appropriately determine the current coding rate and the transmit power by interacting with the environment while guaranteeing the strict QoS requirement. The tasks in the meta-task set are selected according to the channel quality of the M locations with known channel gain samples to ensure the meta-learner can learn the policy with good generalization capability under various environments.

B. Meta-Reinforcement Learning Algorithm

Meta training is a critical procedure for meta-reinforcement learning to obtain a good network initialization parameter. In the following, we will present the meta-reinforcement learning algorithm based on MAML algorithm. The training phase is divided into two levels, i.e., inner-level and outer-level. The inner-level individually optimizes the network parameter on each task gradually. The outer-level aims to update the global parameters with the updated inner-level parameters on the meta-task set. At the beginning of the meta-training phase, each task inherits the global initialized network parameters and then performs inner-level update to update its parameter. The updated parameter of each task will contribute to the outer-level update. It is worth mentioning that the inner-level update can be viewed as a normal update of the previous PPO-based algorithm which aims to find the optimal coding rate and the transmit power for the specified task with a notable difference that here we assume the coding rate and the transmit power are continuous variables instead of discrete variables. In the previous section, we have presented the details of the network update and these formulas can be directly utilized in this part¹. The details of the inner-level update and outer-level update are presented in the following.

For each task \mathcal{T}_i , the agent interacts with the environment based on the initialized meta policy $\pi_{\theta_i} = \pi_{\theta}$. The policy network parameter θ_i is updated as shown in Algorithm 1 every T_g time steps. When the current episode terminates, we employ the updated network to interact with the environment for T time steps and store the trajectory into the replay buffer \mathcal{B}'_i . Once the trajectories of the updated policy networks for all the tasks in \mathcal{N} are collected, we can compute the policy gradient to update the outer-level policy network parameter π_{θ} . The outer-level policy network θ can be updated as follows:

$$\theta \leftarrow \theta + \beta \nabla_{\theta} \sum_{i=1}^N L(\theta_i, \mathcal{B}'_i) \quad (39)$$

where β is the learning rate of the meta-policy, $L(\theta_i, \mathcal{B}'_i)$ is the loss function with respect to θ_i and calculated from the new trajectory in \mathcal{B}'_i as in (26). In the next episode, the updated

¹It is worth mentioning that although the action space types of these two problems are different, PPO is an effective algorithm that can handle both discrete action space and continuous space. The core idea of PPO algorithm is the same while the only difference is that the discrete-PPO utilizes softmax as output action distribution and continuous-PPO adopts normal distribution or beta distribution as the distribution of the action. In this paper, we adopt beta distribution for meta-learning action due to the property of the action space elements being all positive and bounded.

Algorithm 3 MAML-based DRL Algorithm

Input: Randomly initialized policy network parameters θ

for episode = 1, ..., Z **do**

for $\forall \mathcal{T}_i \in \mathcal{T}$ **do**

 Set $\pi_{\theta_i} = \pi_{\theta}$

 Update the inner-level policy network θ_i based on (26) as $\theta_i \leftarrow \theta_i + \alpha \nabla_{\theta_i} L(\theta_i)$ with every T_g time steps by Algorithm 1

 Collect T continuous transition tuples using the updated parameter θ_i to replay buffer \mathcal{B}'_i

end for

 Update the outer-level policy network parameter θ as in (39)

end for

meta parameter θ will be employed as a new initialization for each task \mathcal{T}_i . The overall procedures are summarized in Algorithm 3.

By iteratively executing the inner-level update and the outer-level update, a meta-policy for transmit power and coding rate control can be trained among environments with different channel statistics. Once the meta-policy is trained, the meta-policy can be utilized as an initialization and then optimized for the new task by only executing a few gradient updates.

C. Deployment and Overhead of the Meta-DRL algorithm

The PPO and meta-DRL models are trained offline. More specifically, they are trained based on the virtual environment consisting of the pre-collected historical channel gain samples in dataset \mathcal{D} . The training utilizes the trajectories and the corresponding rewards sampled from the interactions between the agent and the virtual environment before the DRL algorithm deployment. Hence, we can ignore the time consumption of the training process. When deploying the DRL algorithm in a practical setup, we first train the proposed two models offline. The trained PPO-based model can be directly implemented without training but with the requirement of the clustered CKM. The trained meta-DRL model can be regarded as an initialization model for new learning tasks and can be directly implemented. After a small number of gradient update steps, the meta-DRL model can be further improved in a new environment rather quickly.

VI. SIMULATION RESULTS

In this section, we first validate the effectiveness of the PPO-based DRL algorithm for a stationary environment under various QoS constraints. Then we establish a synthetic scenario that constitutes propagation conditions according to standard 3GPP NR Urban Micro-Cell scenario with NLoS models generated by the simulation tool QuaDRiGa [30] for numerical evaluation.

A. DRL-based Transmission Control Algorithm Validation

In this subsection, we will validate the effectiveness of the PPO-based algorithm for the problem (14). For simplicity, we utilize the Rayleigh fading channel with unit

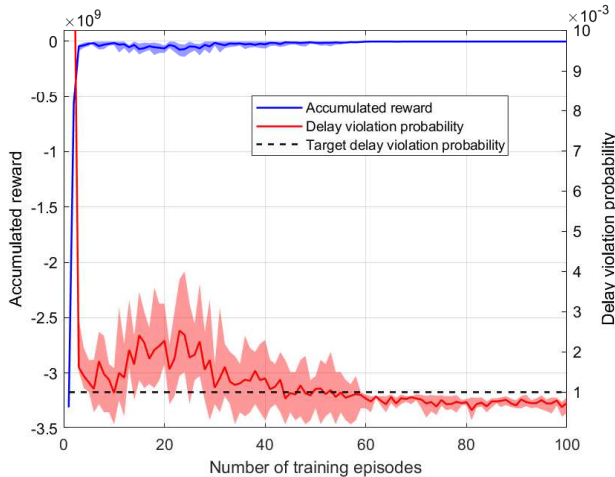


Fig. 2: Learning curves of the PPO algorithm, target DVP $\xi = 10^{-3}$ and $D_{\max} = 5$ slots

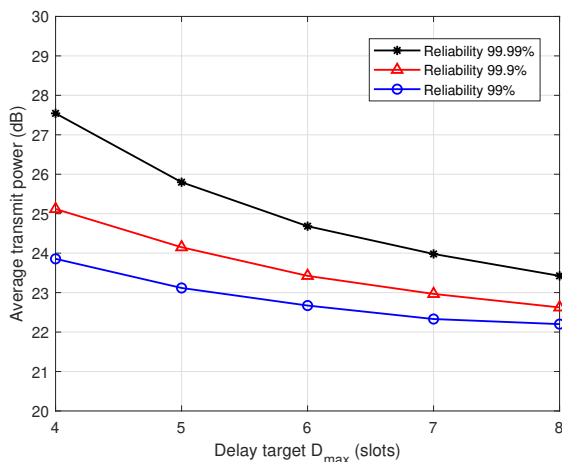


Fig. 3: Impact of reliability and latency.

variance. We use Poisson process to model the stochastic traffic arrival process and the average arrival rate is $\lambda = 800$ bits/slot. The action space consists of $H = 18$ power levels and $G = 20$ outage probability levels. The peak power is set as $p_{\max} = -\frac{2^{\lambda/n} - 1}{\log[1 - (\xi^{D_{\max}}/D_{\max})]}$ empirically. The concrete power levels are assembled as $\mathcal{P} = \{\frac{1}{H}p_{\max}, \frac{2}{H}p_{\max}, \dots, p_{\max}\}$ and the outage probability levels are assembled as $\mathcal{E} = \{\frac{1}{100}, \frac{2}{100}, \dots, \frac{20}{100}\}$. To capture the DVP more accurately, we assume each episode comprises $10/\xi$ steps and there are 100 episodes for training. Regarding PPO, we adopt PPO-clip with a clip ratio $\epsilon = 0.2$. The reward discount factor $\gamma_{\text{DIS}} = 0.99$. Both the actor-network and critic-network learning rates are set to $l_r^a = l_r^c = \alpha = 2 \times 10^{-4}$. T_g is set as 2000 and the minibatch size is $b = 128$. The actor and critic networks are fully connected deep neural networks which have two hidden layers with 128 neurons, and the Tanh function is used as activation.

Firstly, we show the learning curves of the DRL algorithm in Fig. 2 by averaging the accumulated reward and delay violation probability from 10 individual training processes with distinct random environment seeds, and the light color region is the variation region, where the target DVP $\xi = 10^{-3}$,

TABLE II: Environment parameter

Simulation Parameters	Value
Target area \mathcal{Z}	$[-20, 20] \times [-20, 20] \text{ m}^2$
BS location	(0,100) m
BS height	10 m
Device height	1.5 m
Grid spacing	2 m
Transmit power for γ acquisition	0 dBm
Number of total locations L	441
Number of known locations M	110
Number of channel gain samples U	10^3
Channel model	3GPP_3D_UMi_NLOS
Number of paths	12
Central frequency f_c	2.6 GHz
Bandwidth B	200 KHz
Noise power BN_0	-115 dBm
Stochastic arrival distribution	Poisson
Average arrival rate λ	800 bits/slot
Reliability $1 - \xi$	99.9%
Latency D_{\max}	5 slots

(i.e., reliability of 99.9%) and $D_{\max} = 5$ slots. We can see that the accumulated reward increases drastically in the first few episodes and the simulated DVP also decreases drastically, which indicates that there exists a main learning stage. Then in the following, from the 5th-60th episodes, a minor tuning stage exists where the accumulated reward increases slowly and the DVP fluctuates around the DVP target. After the 60th episode, the accumulated reward remains almost constant and the DVP varies within the target DVP threshold which indicates that the policy almost converges. In general, Fig. 2 implies the PPO-based algorithm is capable of solving the transmission control problem with given channel distribution while strictly meeting the QoS requirement.

In Fig. 3, we show the impact of the reliability constraint $1 - \xi$ and the delay target D_{\max} on the average transmit power. Three levels of reliability are considered, namely, $1 - \xi = 99\%$, 99.9% , and 99.99% . The delay target D_{\max} varies from 4 to 8 slots. It is seen that with higher reliability $1 - \xi$ and more stringent delay target D_{\max} , much more average transmit power is required. This observation coincides with the intuition that, the required transmit power increases more rapidly as the QoS requirements become more stringent.

B. Performance Comparison in Synthetic Target Area

In this subsection, we will focus on the formulated problem in (15) with a synthetic environment model generated by QuaDRiGa, a well-known channel model generator, in Matlab. The details of the synthetic environment are summarized in Table II. Specifically, we consider a 21×21 grid area, with a total 441 grids. Among these grids, 110 grids with limited channel gain samples are known at the BS. At each grid, we generated 10^5 channel gain samples. Among them, 10^3 channel gain samples are randomly selected as the known channel gain samples at the BS and will be used for offline CKM establishment and meta-DRL training. The overall 10^5 channel gain samples are used for numerical validation as the virtual environment.

In the following, we first compare the predictive quantile from the CKM and the real quantile of this scenario. Then we show the convergence of the meta-reinforcement learning

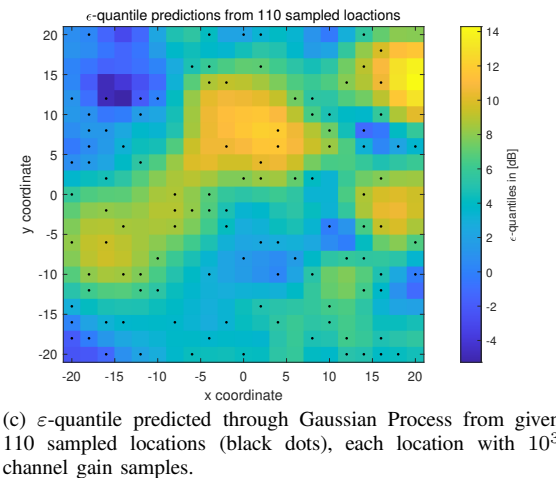
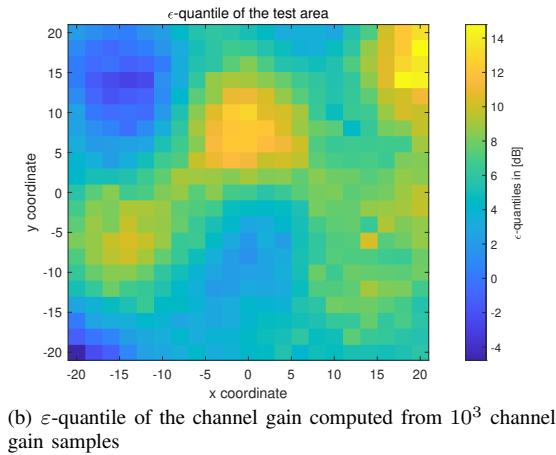
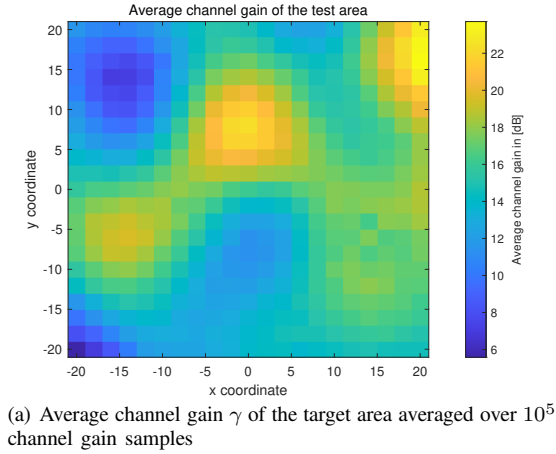


Fig. 4: Average channel gain and the ϵ -quantile comparison of the target area, where $\epsilon = 0.1$

algorithm. Finally, we evaluate the power performance and DVP performance of the power scaling approach in conjunction with the DRL algorithm and the meta-DRL algorithm. Furthermore, the parameters for the base policies training in the proposed power scaling scheme are the same as in subsection VI-A. The only difference is that the peak power cannot be obtained directly but can be calculated as $p_{\max} = \frac{2^{\lambda/n} - 1}{\mathbb{E}\{\gamma|\mathbf{x}\} \log[1 - (\xi^{D_{\max}^{-1}} / D_{\max})]}$. In addition, the number of clusters K is set to be 8 empirically. The network parameters of the meta-DRL algorithm are also the same as the ideal Rayleigh

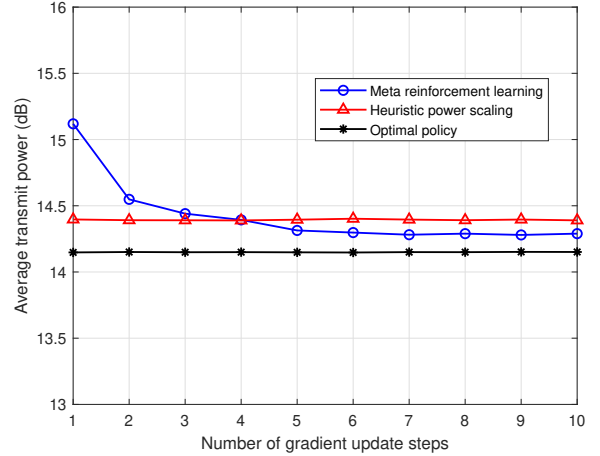


Fig. 5: Adaptability convergence performance of the meta-reinforcement learning

fading channel in subsection VI-A. The number of tasks N is set as 20. In addition, the meta-learning rate β is set as 10^{-3} .

1) *Validation of the predictive CKM:* In Fig. 4(a), we plot the average channel gain of the target area, obtained by averaging the 10^5 channel gain samples of each location. Note that there are three power peaks located around (20, 16), (0, 10), and (-15, -5) and two power valleys around (-20, -20) and (-13, 13) for the particular realization of our simulated environment. In Fig. 4(b), we plot the 0.1-quantiles of the known channel gain samples. We can see that the overall shape is similar to the average channel gain with a rough grid and different average values. Fig. 4(c) depicts the predicted 0.1-quantile CKM through 110 locations marked as dots on the map. We can see that this map is also similar to Fig. 4(b) except for those locations far away from the observed locations in \mathcal{D} . It is also seen that the predicted 0.1-quantile CKM is quite similar to the real one due to the space consistency through continuous Gaussian process interpolation.

2) *Convergence validation of the meta-DRL algorithm:* To show the adaptability of the meta-reinforcement learning algorithm, we first show the convergence performance of the meta-policy in a Rayleigh fading scenario with average channel gain $\mathbb{E}\{\gamma\} = 10\text{dB}$ as the gradient update steps increase in Fig. 5. Here the gradient is updated every $T_{\text{ap}} = 1000$ time slots as (26) in the adaptation stage. Simultaneously, we also show the performance of the power scaling solution by selecting an appropriate base location. The average transmit power of the meta-reinforcement learning algorithm initialization without parameter update conducted from the interaction with the environment does not outperform the proposed power scaling scheme. As the number of gradient updates increases, the average transmit power decreases drastically and then gradually converges within 10 gradient update steps and outperforms the proposed power scaling scheme. The performance of the power scaling solution and the optimal policy are almost constant since these two schemes can not learn from the new environment.

3) *Validation of the proposed solutions:* In order to evaluate the performance of the two solutions, we introduce two bench-

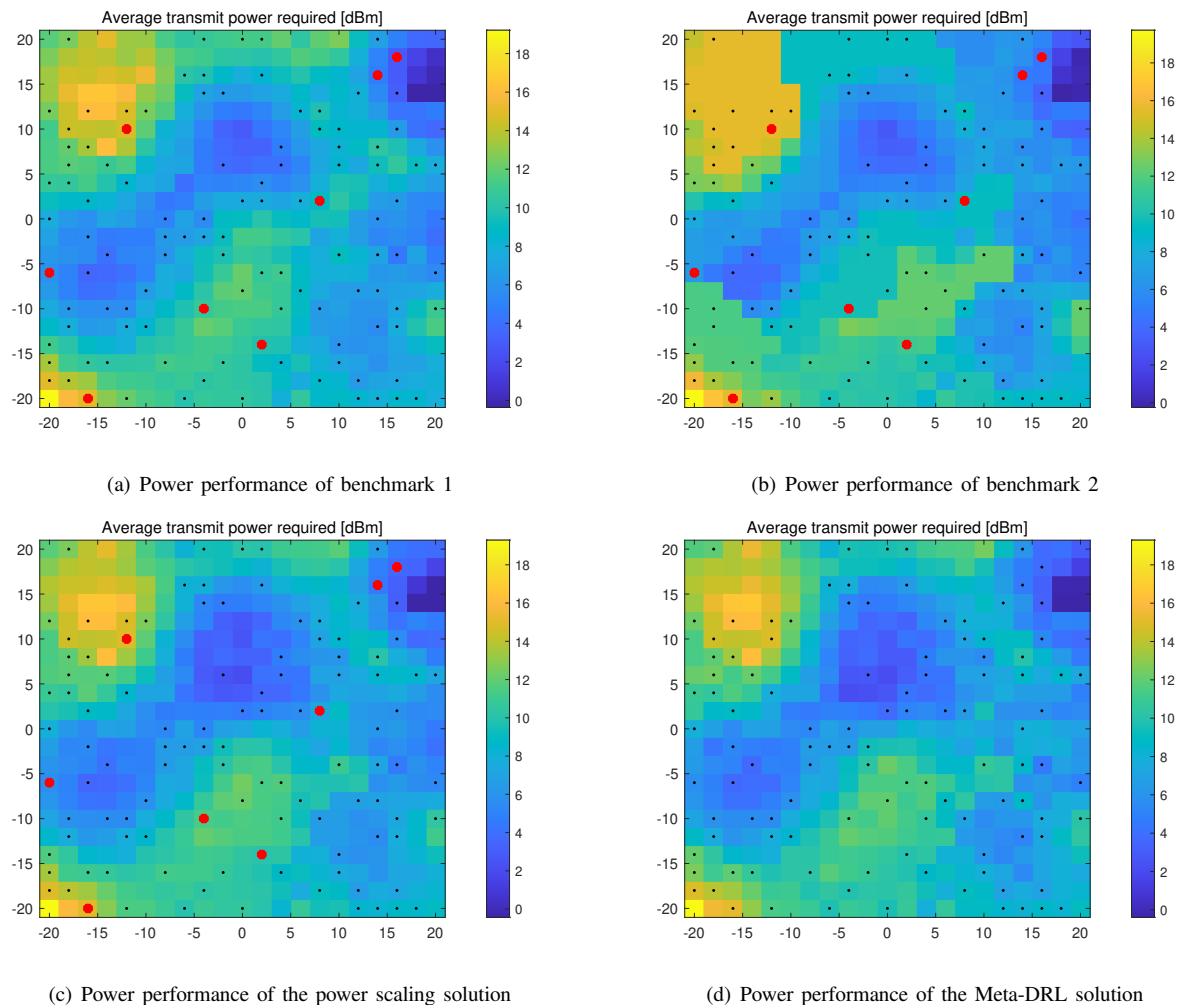


Fig. 6: Power performance comparison with a target DVP $\xi = 10^{-3}$ and $D_{\max} = 5$ slots, the red dots stand for the $K = 8$ base locations with trained policy networks

mark schemes for comparison. The details of these solutions are summarized as follows:

- Meta-DRL solution: This solution shows the adaptation result of the meta-DRL solution as in Algorithm 3 after 10 gradient update steps adaptation in the new locations.
- Power scaling solution: This solution shows the result of power scaling scheme through the improved K -means clustering.
- Benchmark 1: This solution also shows the result of the power scaling scheme, but rather than the improved K -means clustering method, it simply uses the policy from the nearest base location on the map for power scaling.
- Benchmark 2: This solution directly utilizes the nearest base location's policy for the current location on the map without any adaptation.

Fig. 6 depicts the transmit power performance of these four schemes. Here we randomly choose one channel gain sample from the 10^5 generated channel gain samples to interact with the agent in each time slot and calculate the corresponding average transmit power and the overall DVP over 10^5 slots for the locations within the target area. It is worth mentioning that we still use black dots to stand for the sampled locations

and red dots to stand for base locations on the map in Fig. 6 and Fig. 7. It is observed that the transmit power maps of these four schemes are roughly complementary to the average channel gain map in Fig. 4(a). The power performance of the two solutions and benchmark 1 are quite similar. While the performance of benchmark 2 is worse than the above 3 solutions.

In Fig 7, we show the DVP performance maps of the four schemes. Specifically, we use different colors for different orders of magnitude of the DVP. For benchmark 1, with the help of the power scaling scheme, the DVP constraint is improved greatly, and only a small amount of locations' DVP constraints are violated by one order of magnitude as depicted in Fig. 7(a). For benchmark 2, DVP constraints of more than half of the locations within the target area are not met as depicted in Fig. 7(b). The DVP constraints are violated by a few orders of magnitude. More specifically, most of these locations under DVP constraints are around the base-policy locations, which indicates the spatial correlation of the channel distribution. For the proposed power scaling scheme in Fig. 7(c), the DVP performance is better than benchmark 1 due to the improved K -means clustering. Finally, the DVP

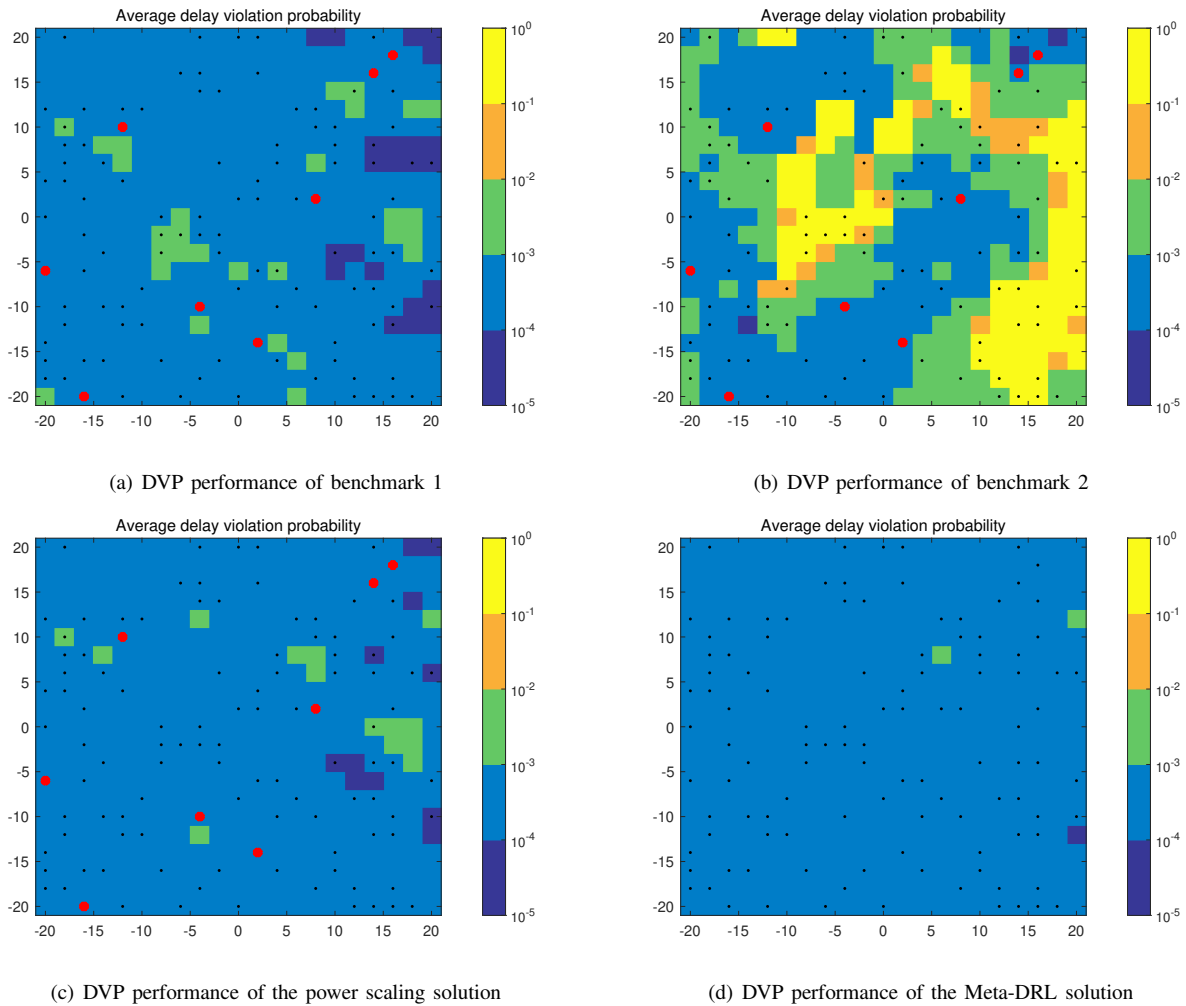


Fig. 7: DVP performance comparison with a target DVP $\xi = 10^{-3}$ and $D_{\max} = 5$ slots, the red dots stand for the $K = 8$ base locations with trained policy networks

performance of the meta DRL based algorithm outperforms the DRL-based power scaling scheme, and only two locations' DVP constraints are violated as shown in Fig. 7(d).

As a result, we calculate the average transmit power and corresponding availability across the target area through different solutions in Table III. The average transmit power is calculated by averaging the long-term average transmit power across the target area through different solutions. The availability is calculated by the probability that the QoS (i.e., reliability and latency) of users can be satisfied in a wireless network. In the space domain, it is the ratio of the covered area, within which the QoS can be satisfied, to the total service area. Furthermore, to be more persuasive, we also show the 95% confidence interval of the availability by normal approximation. This confidence interval is an interval estimate of a success probability calculated from the outcome of the overall $L = 441$ binomial experiments, i.e., DVP performance evaluation. In general, we can conclude that by directly applying the $K=8$ trained networks into the considered area without transmit power scaling, the overall availability only achieves 44.22%. When the CKM is established, the transmit power scaling from most nearby base-policy can significantly enhance the

availability to 93.42%. In the meanwhile, the average transmit power is reduced by about 14%. When both the improved K -means clustering and transmit power scaling are employed, both the transmit power and availability are slightly improved, which implies the effectiveness of the K -means clustering. Finally, we can observe that the performance of the meta-DRL method can achieve the best power performance and the highest availability, which shows the effectiveness of the meta-DRL algorithm.

VII. CONCLUSION

We have investigated the transmission control adaptation problem for mission-critical IoT systems with URLLC in a target area exploiting the channel gain samples of a few locations known at the BS. We have first formulated a transmission control problem for a specific location with known channel gain samples while guaranteeing the stringent QoS requirement of URLLC by dynamically determining the transmit power and coding rate. This was followed by a policy adaptation problem for the users across the target area with various channel statistics under the same QoS requirement. We have first utilized a PPO-based algorithm to solve the

TABLE III: Performance comparison

Solutions	Meta-DRL	Power scaling	Benchmark1	Benchmark2
Average transmit power	8.978 mW (9.532 dBm)	9.034 mW (9.559 dBm)	9.378 mW (9.721 dBm)	10.689 mW (10.289 dBm)
Availability observation	99.55%	96.83%	92.97%	44.22%
95% confidence interval of the availability	98.93% ~ 100%	95.19% ~ 98.47%	90.62% ~ 95.38%	39.58% ~ 48.86%

transmission control problem for a specific location. This has been supplemented by a power scaling scheme based on the above PPO-based algorithm via CKM for the policy adaptation problem without re-training. Our second proposal is MAML-based meta-reinforcement learning algorithm based on the PPO-based algorithm, which can effectively train a meta policy. This meta policy can adapt quickly to new environments within a few gradient updates after interacting with the realistic environment. The numerical results have validated the effectiveness of the PPO-based algorithm for the transmission control problem under various QoS requirements. It has been shown that the two proposals can solve the transmission control adaptation problem with high QoS availability compared to the benchmark scheme without power scaling. The immediate future work is a generalization of the proposed methods to the base stations and UEs with multiple antennas. Furthermore, future work can also take the following two practical impacts into account: The first is the user mobility within the target area. The second is maintaining the dynamic CKM, since the realistic channel models usually comprise of non-static propagation environments.

REFERENCES

- [1] P. Popovski, Č. Stefanović, J. J. Nielsen, E. de Carvalho, M. Angelichinoski, K. F. Trillingsgaard, and A. Bana, "Wireless access in ultra-reliable low-latency communication (URLLC)," *IEEE Trans. Commun.*, vol. 67, no. 8, pp. 5783–5801, Aug. 2019.
- [2] O. L. A. López, N. H. Mahmood, M. Shehab, H. Alves, O. M. Rosabal, L. Marata, and M. Latva-Aho, "Statistical tools and methodologies for ultrareliable low-latency communication—a tutorial," *Proceedings of the IEEE*, vol. 111, no. 11, pp. 1502–1543, Nov. 2023.
- [3] R. Singh, A. Kaushik, W. Shin, M. D. Renzo, V. Sciancalepore, D. Lee, H. Sasaki, A. Shojaeifard, and O. A. Dobre, "Towards 6G evolution: Three enhancements, three innovations, and three major challenges," *arXiv: 2402.10781*, 2024.
- [4] ITU-R, "Framework and overall objectives of the future development of int for 2030 and beyond," Jun. 2023.
- [5] M. Bennis, M. Debbah, and H. V. Poor, "Ultrareliable and low-latency wireless communication: Tail, risk, and scale," *Proceedings of the IEEE*, vol. 106, no. 10, pp. 1834–1853, Oct. 2018.
- [6] C. She, C. Sun, Z. Gu, Y. Li, C. Yang, H. V. Poor, and B. Vucetic, "A tutorial on ultrareliable and low-latency communications in 6G: Integrating domain knowledge into deep learning," *Proc. IEEE*, vol. 109, no. 3, pp. 204–246, Mar. 2021.
- [7] V. N. Swamy, P. Rigge, G. Ranade, B. Nikolić, and A. Sahai, "Wireless channel dynamics and robustness for ultra-reliable low-latency communications," *IEEE J. Sel. Areas in Commun.*, vol. 37, no. 4, pp. 705–720, Apr. 2019.
- [8] M. Angelichinoski, K. F. Trillingsgaard, and P. Popovski, "A statistical learning approach to ultra-reliable low latency communication," *IEEE Trans. Commun.*, vol. 67, no. 7, pp. 5153–5166, Jul. 2019.
- [9] T. Kallehauge, P. Ramírez-Espinosa, A. E. Kalør, C. Biscio, and P. Popovski, "Predictive rate selection for ultra-reliable communication using statistical radio maps," in *Proc. IEEE Global Commun. Conf. (Globecom)*, Dec. 2022, pp. 4989–4994.
- [10] D. Qiao, M. Gursoy, and S. Velipasalar, "Throughput-delay tradeoffs with finite blocklength coding over multiple coherence blocks," *IEEE Trans. Commun.*, vol. 67, no. 8, pp. 5892–5904, Aug. 2019.
- [11] H. Peng and M. Tao, "Effective capacity of URLLC over parallel fading channels with imperfect channel state information," *China Commun.*, vol. 21, no. 5, pp. 45–63, May 2024.
- [12] S. Schiessl, H. Al-Zubaidy, M. Skoglund, and J. Gross, "Delay performance of wireless communications with imperfect csi and finite-length coding," *IEEE Trans. Commun.*, vol. 66, no. 12, pp. 6527–6541, Dec. 2018.
- [13] C. Liu and M. Bennis, "Ultra-reliable and low-latency vehicular transmission: An extreme value theory approach," *IEEE Commun. Lett.*, vol. 22, no. 6, pp. 1292–1295, Jun. 2018.
- [14] H. Peng, T. Kallehauge, M. Tao, and P. Popovski, "Power and rate adaptation for URLLC with statistical channel knowledge and HARQ," *IEEE Wireless Commun. Lett.*, vol. 12, no. 12, pp. 2148–2152, Dec. 2023.
- [15] R. Levie, c. Yapar, G. Kutyniok, and G. Caire, "Radiounet: Fast radio map estimation with convolutional neural networks," *IEEE Trans. Wireless Commun.*, vol. 20, no. 6, pp. 4001–4015, Mar. 2021.
- [16] S. Bi, J. Lyu, Z. Ding, and R. Zhang, "Engineering radio maps for wireless resource management," *IEEE Wireless Commun.*, vol. 26, no. 2, pp. 133–141, Apr. 2019.
- [17] De Lima, Carlos et. al., "Convergent communication, sensing and localization in 6G systems: An overview of technologies, opportunities and challenges," *IEEE Access*, vol. 9, pp. 26 902–26 925, 2021.
- [18] Y. Zeng and X. Xu, "Toward environment-aware 6G communications via channel knowledge map," *IEEE Wireless Commun.*, vol. 28, no. 3, pp. 84–91, Jun. 2021.
- [19] Y. Zeng, J. Chen, J. Xu, D. Wu, X. Xu, S. Jin, X. Gao, D. Gesbert, S. Cui, and R. Zhang, "A tutorial on environment-aware communications via channel knowledge map for 6G," *IEEE Communications Surveys & Tutorials*, pp. 1–1, 2024.
- [20] G. Durisi, T. Koch, and P. Popovski, "Toward massive, ultrareliable, and low-latency wireless communication with short packets," *Proceedings of the IEEE*, vol. 104, no. 9, pp. 1711–1726, Sep. 2016.
- [21] W. Yang, G. Durisi, T. Koch, and Y. Polyanskiy, "Quasi-static multiple-antenna fading channels at finite blocklength," *IEEE Trans. Inf. Theory*, vol. 60, no. 7, pp. 4232–4265, Jul. 2014.
- [22] H. Peng, M. Tao, T. Kallehauge, and P. Popovski, "Power adaptation in URLLC over parallel fading channels in the finite blocklength regime," in *Proc. IEEE Global Commun. Conf. (Globecom)*, Dec. 2022, pp. 1819–1824.
- [23] A. Anand and G. de Veciana, "Resource allocation and HARQ optimization for URLLC traffic in 5G wireless networks," *IEEE J. Sel. Areas in Commun.*, vol. 36, no. 11, pp. 2411–2421, Nov. 2018.
- [24] J. Schulman, F. Wolski, P. Dhariwal, A. Radford, and O. Klimov, "Proximal policy optimization algorithms," *arXiv: 1707.06347*, 2017.
- [25] J. Schulman, S. Levine, P. Moritz, M. I. Jordan, and P. Abbeel, "Trust region policy optimization," *arXiv: 1502.05477*, 2015.
- [26] T. Kallehauge, A. E. Kalør, P. Ramírez-Espinosa, M. Guillaud, and P. Popovski, "Delivering ultra-reliable low-latency communications via statistical radio maps," *IEEE Wireless Commun.*, vol. 30, no. 2, pp. 14–20, Apr. 2023.
- [27] A. Stuart and K. Ord, *Kendall's advanced theory of statistics, distribution theory*. John Wiley & Sons, 2010, vol. 1.
- [28] C. K. Williams and C. E. Rasmussen, *Gaussian processes for machine learning*. MIT press Cambridge, MA, 2006, vol. 2, no. 3.
- [29] C. Finn, P. Abbeel, and S. Levine, "Model-agnostic meta-learning for fast adaptation of deep networks," *arXiv: 1703.03400*, 2017.
- [30] S. Jaeckel, L. Raschkowski, K. Börner, L. Thiele, F. Burkhardt, and E. Eberlein, "Quasi deterministic radio channel generator user manual and documentation," *Fraunhofer Heinrich Hertz Inst.*, 2017.